

# Bidirectional Dual Active Half-Bridge Converter Integrated High Power Factor Correction

AnhTuan Ngo , Kwanghee Nam

Electronics and Electrical Engineering Department, POSTECH, Pohang, Korea

## Abstract

**Abstract**—A bidirectional dual active converter with the power factor control capability is proposed as a battery charger. The source side half-bridge acts as a PWM converter that maintains the unity power factor. The battery side half-bridge converter acts as a dual active bridge (DAB) together shares the same DC link voltage with PWM converter. The imbalance voltage phenomenon is eliminated by employing asymmetric duty cycle technique. Simulation results are included to verify theoretical analysis.

**Index Terms**—Bidirectional half-bridge converter, battery charger, power factor correction, asymmetric duty ratio.

## I. INTRODUCTION

Due to air pollution and exhaustion of fossil fuels, nowadays, an AC-DC converter is an attractive solution for many applications. Conventionally, the front-end is an active single-phase or three-phase pulse-width modulation (PWM) rectifier to obtain power factor correction [2], [12], [14]. In [11], several topologies for both bidirectional and unidirectional converters have been reviewed.

In this work, a new bidirectional single-phase based on half-bridge converter is proposed for battery charger applications. The input current waveform can shape source voltage while energy transferred to battery package. The unbalanced-voltage problem is solved by utilizing asymmetric duty control technique [6], [5]. A 300 W converter was simulated to support the study. The introduced converter is very promising for low-power applications, especially bidirectional battery charger.

## II. OPERATION PRINCIPLE OF PROPOSED CONVERTER

Fig.1 shows the single-phase circuit of proposed converter. A PWM rectifier connects to 60 Hz source voltage and maintain nearly unity power factor. This rectifier shares the same DC link voltage with a DAB converter which is constituted by two half-bridge converters laid back-to-back through a transformer. The converter can transfer energy in a bidirectional manner: from the source to load and inversely from the load to the source.

For better understanding, the operations of PWM converter and dual active half-bridge converter are explained separately.

### A. PWM Converter for Power Factor Correction

To achieve unity power factor, two switches  $S_1$ ,  $S_2$  are turned-on and -off complementarily. Voltages across capacitors

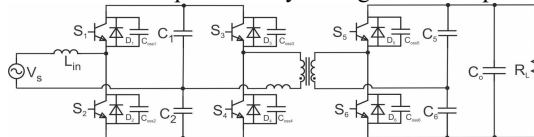


Fig. 1 The proposed topology for battery charger.

$V_{C1}$  and  $V_{C2}$  are larger than the peak value of source voltage  $v_s$ . Due to the symmetric, the operating principle in positive half-line cycle is presented with  $D$  defined as duty ratio of  $S_2$ .

**When  $S_2$  is on:** the input current  $i_L$  steeply increases because positive voltage ( $v_s + V_{C2}$ ) applies directly to inductor. Boost inductor  $L_{in}$  is energized and stores energy from the source. Current  $i_L$  is denoted by

$$i_L(t) = i_L(0) + \frac{v_s + V_{C2}}{L_{in}} t \quad (1)$$

This interval duration is  $DT_s$ .

**When  $S_1$  is on:** input current decreases linearly from its peak value due to negative voltage on inductor. The stored energy is released to capacitor and the load. Boost current is given by

$$i_L(t) = i_L(DT_s) + \frac{-v_s + V_{C1}}{L_{in}} (t - DT_s) \quad (2)$$

From the volt-sec balance condition, duty cycle  $D$  is determined

$$v_s = V_{C1} - D(V_{C1} + V_{C2}) \quad (3)$$

To obtain unity power factor, the duty  $D$  is modulated by hysteresis current control (HCC) [12] or sinusoidal PWM (SPWM) [2], [4].

The main drawback of single-phase based on half-bridge converter is the unbalanced-voltage between  $v_{C1}$  and  $v_{C2}$ .

This causes input current distortions and harmonics. Several methods to eliminate this fluctuation phenomenon have been reported [2], [4], [12], [13]. In this paper, asymmetric duty technique is employed and thoroughly discussed later.

### B. Dual Active Half-Bridge Converter with Asymmetric Duty Control

All the parameters are referred to secondary side of transformer. The gating-pulse signals, voltages in both sides of transformer and leakage current of DAHB are drawn in Fig.2.

One more variable,  $\theta$ , is added to the control scheme to feature asymmetric duty control. Then on-time duration of the primary side switches are  $T_{S3} = \pi + \theta$  and  $T_{S4} = \pi - \theta$  while in secondary side  $T_{S5} = T_{S6} = \pi$ . The equivalent circuits of DAHB with asymmetric duty technique shown in Fig.3 are divided in six detailed stages for determining the charging and discharging intervals of capacitors. The operating principle is presented as follow.

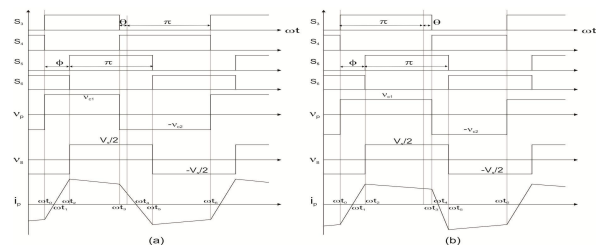


Fig. 2 Key waveforms of DAHB converter with asymmetric duty cycle: (a)  $\theta$  is negative, (b)  $\theta$  is positive.

**Stage 1 ( $\omega t_0 \div \omega t_1$ ):** At  $\omega t_0$ ,  $S_4$  is turned off and  $S_3$  is turned on. The current flows through  $D_3$  and  $D_6$ , the anti-parallel diodes of  $S_3$  and  $S_6$ , respectively. In this stage, both capacitors  $C_1$  and  $C_4$  are charged by stored energy in  $L_{lk}$ . The current  $i_s$  is given by

$$i_s(\omega t) = \frac{v_{C1} + V_o / 2}{\omega L_{lk}} \omega t + i_s(\omega t_0) \quad (4)$$

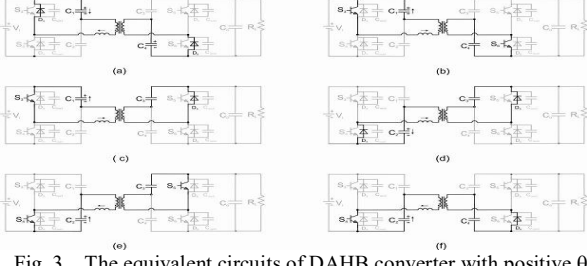


Fig. 3 The equivalent circuits of DAHB converter with positive  $\theta$ .

**Stage 2 ( $\omega t_1 + \omega t_2$ )** : the  $i_s$  current changes its direction from negative to positive value and discharges both capacitors  $C_1$  and  $C_4$ .  $i_s$  is the same as (4). Two switches  $S_3$  and  $S_6$  are conducting as drawn in Fig.3(b). This stage is ended when it reaches its peak positive value.

**Stage 3 ( $\omega t_2 + \omega t_3$ )** :  $i_s$  flows through  $S_3$  and  $D_5$  due to ON state of  $S_6$  at  $\omega t_2$ . During this interval,  $i_s$  charges and discharges  $C_3$ ,  $C_1$ , respectively. Voltage applies on inductor  $L_{lk}$  is  $(v_{C1} - V_o/2)$  and  $i_s$  is denoted by

$$i_s(\omega t) = \frac{v_{C1} - V_o/2}{\omega L_{lk}}(\omega t - \phi) + i_s(\omega t_2) \quad (5)$$

Note that the amount of current discharges  $C_1$  can be controlled by regulating the period of this stage.

**Stage 4 ( $\omega t_3 + \omega t_4$ )** : This stage start from the time when  $S_3$  is turned off and  $S_4$  is turned on. The current  $i_s$  flows through two body parallel diodes  $D_4$  and  $D_5$  as shown in Fig.3(d) and decreases due to voltage applies on leakage  $L_{lk}$  is negative. During this interval, the stored energy in  $L_{lk}$  charges up both capacitor  $C_2$  and  $C_3$ .  $i_s$  is calculated as

$$i_s(\omega t) = \frac{-v_{C2} - V_o/2}{\omega L_{lk}}(\omega t - \pi - \phi) + i_s(\omega t_3) \quad (6)$$

This stage is terminated when  $i_s$  equals zero at  $\omega t_4$ .

**Stage 5 ( $\omega t_4 + \omega t_5$ )** :  $i_s$  increases from zero in negative direction through  $S_4$  and  $S_5$ . Because of the changing in  $i_s$  flow, both capacitors  $C_2$  and  $C_3$  are discharging for energizing inductor  $L_{lk}$ . The current is the same as (6) in this interval. This period is ended when  $i_s$  reaches its negative peak value.

**Stage 6 ( $\omega t_5 + \omega t_6$ )** : The current is continues discharging  $C_2$  and charging  $C_4$  through  $S_4$  and  $D_6$ . In this stage,  $i_s$  is indicated by

$$i_s(\omega t) = \frac{v_{C2} - V_o/2}{\omega L_{lk}}(\omega t - \pi - \phi - \theta) + i_s(\omega t_5) \quad (7)$$

This interval finishes at  $\omega t_6$ .

In case of asymmetric duty control, the boundary condition for leakage inductor current is  $i(\omega t_6) = i(\omega t_6)$ , then results in

$$v_{C1}(\phi + \theta) = v_{C2}(\pi - \theta) \quad (8)$$

$$\text{or } \theta = -\frac{(v_{C1} - v_{C2})}{(v_{C1} + v_{C2})} \pi = -\frac{(v_{C1} - v_{C2})}{V_{dc}} \pi = -\frac{\Delta v}{V_{dc}} \pi \quad (9)$$

The additional angle  $\theta$  depends linearly on the difference voltage  $\Delta v$ , i.e., between two capacitors  $C_1$ ,  $C_2$  while the DC link voltage is assuming constant.

With the same procedure as symmetric half-bridge converter [3], [10], [6], the output power is calculated as

$$P_o = \frac{V_o}{8\pi\omega L_{lk}} \left[ \frac{v_{C1}}{n} (-2\phi^2 - \pi^2 - \theta^2 + 4\pi\phi - 2\pi\theta + 4\theta\phi) + \frac{v_{C2}}{n} (-2\phi^2 + \pi^2 - \theta^2 - 2\pi\theta + 4\theta\phi) \right] \quad (10)$$

In the steady state,  $v_{C1} = v_{C2} = nV_o/2$ . The output power is rewritten

$$P_o = P_c + P_a = \frac{V_o^2}{4\pi\omega L_{lk}} \phi(\pi - \phi) + \frac{V_o^2}{8\pi\omega L_{lk}} [4\theta\phi - \theta^2 - 2\theta\phi] \quad (11)$$

It should be noted from (11) that the output power  $P_o$  constitutes of two parts:  $P_c$ , caused by conventional phase-shift control [3], [9], [7], [6] and  $P_a$ , due to asymmetric duty cycle.

The control block diagram of whole system is shown as following in Fig.4 .

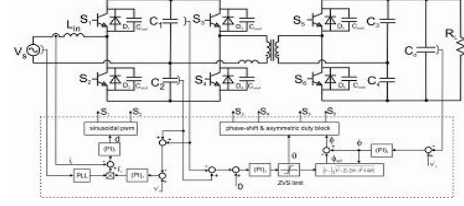


Fig. 4 The entire control block diagram of proposed converter.

The conventional control for power factor correction requires two proportional-integral (PI) controllers: one for inner current loop and the other for DC link voltage loop. Traditional PI is employed to adjust output power. The angle  $\theta$  is used for curing imbalance voltage. A PI controller can be adopted to that controller because  $\theta$  increases linearly with the voltage difference  $\Delta v$ . The decoupling term between two-later PI controllers is derived as same technique as in [6].

### III. SIMULATION AND EXPERIMENT RESULTS

A 300 W, 90 V input voltage converter was simulated in ANSOFT SIMPLORER 6.0. The simulation results are shown in Fig.6. Compared to Fig.5 where the unbalanced-voltages across capacitors are in range of 0 to 25 V, the differences of two those capacitors with proposed method are very small, in range of  $-0.25 \div 0.25$  V while input current shaping input voltage.

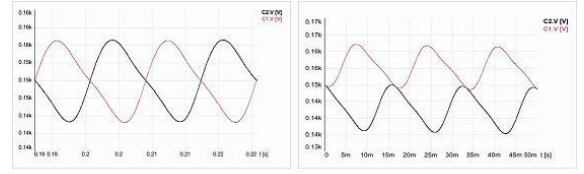


Fig. 5 Unbalanced-voltage phenomenon between two capacitors: (a) SPWM method, (b) HCC method.

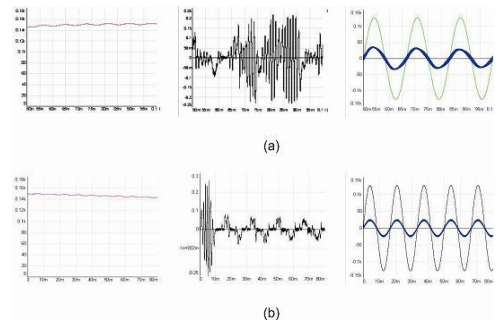


Fig. 6 Voltage, difference of voltage between two capacitors and input voltage and current waveforms: (a) SPWM method, (b) HCC method.

Experiments are now conducting to support the theoretical analysis and will be reported later.

### IV. CONCLUSION

A new battery charger for low-power applications based on half-bridge converter has been introduced in this paper. The converter can operate near unity power factor while imbalance voltage phenomenon is eliminated by employing asymmetric duty technique. The effectiveness of proposed converter was verified by simulation results.

## REFERENCES

- [1] M. Antchev, M. Petkova, V. Gurgulitsov, and H. Antchev. Study of a single-phase bidirectional ac/dc converter with a high power factor. In EUROCON 2009, EUROCON '09. IEEE, pages 1521–1527, May 2009.
- [2] J. Boys and A. Green. Current-forced single-phase reversible rectifier. *Electric Power Applications*, IEE Proceedings B, 136(5):205–211, Sept. 1989.
- [3] R. De Doncker, D. Divan, and M. Kheraluwala. A three-phase soft-switched high-power-density dc/dc converter for high-power applications. *Industry Applications*, IEEE Transactions on, 27(1):63–73, 1991.
- [4] R. Ghosh and G. Narayanan. A simple analog controller for single-phase half-bridge rectifier. *Power Electronics*, IEEE Transactions on, 22(1):186–198, 2007.
- [5] P. Imbertson and N. Mohan. Asymmetrical duty cycle permits zero switching loss in pwm circuits with no conduction loss penalty. *Industry Applications*, IEEE Transactions on, 29(1):121–125, 1993.
- [6] J. Kim, I. Jeong, and K. Nam. Asymmetric duty control of the dual-active-bridge dc/dc converter for single-phase distributed generators. In Energy Conversion Congress and Exposition, 2009. ECCE 2009. IEEE, pages 75–82, 2009.
- [7] F. Krismer and J. Kolar. Accurate power loss model derivation of a high-current dual active bridge converter for an automotive application. *Industrial Electronics*, IEEE Transactions on, 57(3):881–891, march 2010.
- [8] G. Moschopoulos, M. Qiu, H. Pinheiro, and P. Jain. Pwm full-bridge converter with natural input power factor correction. *Aerospace and Electronic Systems*, IEEE Transactions on, 39(2):660–674, 2003.
- [9] G. Oggier, G. Garcia, and A. Oliva. Switching control strategy to minimize dual active bridge converter losses. *Power Electronics*, IEEE Transactions on, 24(7):1826–1838, July 2009.
- [10] F. Peng, H. Li, G.-J. Su, and J. Lawler. A new zvs bidirectional dc-dc converter for fuel cell and battery application. *Power Electronics*, IEEE Transactions on, 19(1):54–65, 2004.
- [11] B. Singh, B. Singh, A. Chandra, K. Al-Haddad, A. Pandey, and D. Kothari. A review of single-phase improved power quality ac-dc converters. *Industrial Electronics*, IEEE Transactions on, 50(5):962–981, oct. 2003.
- [12] R. Srinivasan and R. Oruganti. A unity power factor converter using half-bridge boost topology. *Power Electronics*, IEEE Transactions on, 13(3):487–500, May 1998.
- [13] G.-J. Su, D. Adams, and L. Tolbert. Comparative study of power factor correction converters for single phase half-bridge inverters. In *Power Electronics Specialists Conference*, 2001. PESC. 2001 IEEE 32<sup>nd</sup> Annual, 2001.
- [14] N. Tan, T. Abe, and H. Akagi. A 6-kw, 2-kwh lithium-ion battery energy storage system using a bidirectional isolated dc-dc converter. In *Power Electronics Conference (IPEC)*, 2010 International, pages 46–52, June 2010.